IOP Conference Series: Earth and Environmental Science

PAPER • **OPEN ACCESS**

Study on mechanical properties of triaxial unloading of granite under pore pressure

Study on mechanical properties of triaxial unloading of granite under pore pressure

Jianxi Ren, Mengchen Yun* and Kun Zhang

College of Architecture and Civil Engineering, Xi´an University of Science and Technology, Xi'an Shaanxi,710054, China.

*Corresponding author's e-mail: 18204058031@stu.xust.edu.cn

Abstract. This research analyzes the strength and deformation characteristics of rock samples under varying pore pressures during the unloading process. By using fine-grained granite from Western China as the research exemplar, laboratory tests of triaxial unloading under pore pressure are conducted by utilizing the unloading confining pressures method without changing the axial pressure. Pore pressure is tested with a design value of 5 MPa. When the confining pressures are released at 35, 25, 15, and 5 MPa, the pore pressures drainage valve are opened, and the mechanical properties of fine-grained granite under pore pressures are analyzed. The following results are obtained. After unloading at different confining pressures, pore pressure has an evident influence on the stress–strain curve of the rock sample. The bearing capacity of the rock sample decreases. The hole pressure has a significant effect on the ring and volume deformation in the unloading process. Consequently, the evident deformation and damage are generated immediately after unloading to 25 MPa. Under the condition of constant pore pressure for a long time, numerous tension fractures are distributed around the main shear fracture owing to the promotion of pore pressure on the fracture opening. Hence, an evident swelling phenomenon occurs in the rock sample.

1. Introduction

The majority of the hydropower explanation built in Northwest China are located between high and steep mountains. During the construction process, long water diversion tunnels and supporting treatments of various large slopes are often frequently occurs [1]. Therefore, pore water pressures in rocks that cause deformation and failure characteristics during excavation is an urgent problem that should be solved [2–4]. In geotechnical engineering, the surrounding rock mass is in unloading state during the mining and construction of underground caverns and tunnels. The mechanical properties of rocks under an unloading state are different from those under conventional loading. Thus, the influence of osmotic pressure on rock failure under unloading condition is studied indepth. Accordingly, the considering factors are applied to understand the failure mechanism of confining pressure under high stress water pressure, judge the stability of the confining pressure, prevent the occurrence of water seepage and water gushing in the tunnel, and determine a safe, economic, and effective construction scheme [5,7].

The deformation of rock mass under the coupling effect of seepage stress and unloading mechanics of rock mass has been studied extensively and yielded substantial results. Ki-Bok Min [8] conducted a series of numerical experiments and calculated the permeability changes of simulated fractured rock mass under different loading conditions. Huang et al. [9] established a constitutive equation of post peak brittle section of unloading rock by using strain softening theory, and studied the entire stress–

strain process curve and fracture characteristics of rock under unloading condition. Evan et al. [10] analyzed the sensitivity of hydraulic conductivity of fractured rock, groundwater flow path, shear stress, and normal fracture stiffness to a series of deviatoric stress states. Zhang et al. [11] found that the permeability of rock samples changed in a “V” shape during triaxial compression, and established a strain softening model of rock samples under confining pressure. Wang et al. [12] conducted seepage stress coupling tests under different confining and pore pressures, and analyzed the variation law of rock permeability in the fracture process. Deng et al. [13] performed triaxial unloading tests under different confining pressures and different pore pressures, and determined the influence of low pore pressure on the unloading mechanical properties of rock samples. Li et al. [14] used microscopic infrared spectroscopy imaging technology to determine the influence law of pores and fractures in rocks and different media in rocks on seepage performance. Chen et al. [15] conducted triaxial loading and unloading tests on granite, compared and analyzed the energy change trend of each stage before the peak, and determined the relationship between the failure of rock bridge, accumulation and release of energy. Huang et al. [16] used the non-Darcy flow equation as the basis in deducing and verifying the relationship between the permeability coefficient and water pressure of fractured rock mass under high water pressure. Xie et al. [17] performed uniaxial and triaxial compression tests on soft rocks with different water contents, and analyzed the microstructure of soft rocks using X-ray diffraction technology. Li et al. [18] quantitatively analyzed the influence of water on the unloading mechanical properties of shale from a macroscopic perspective by using unloading confining pressure tests with varying water saturation coefficients. The research results have certain significance for correctly understanding the fracture mechanism and deformation characteristics of surrounding rock mass during tunnel excavation in rich water mountainous area.

Numerous studies have been conducted on the variation of permeability in the rock fracture process. However, only minimal researches have been conducted on the changes in rock sample strength and deformation characteristics caused by different pore pressure stages. The current study conducts unloading tests of fine-grained granite under different pore pressure stages. The response degrees of axial, circumferential, and volume deformations to the confining pressure unloading process under different pore pressure stages are obtained. The research results have significance for correctly understanding the fracture mechanism and deformation characteristics of surrounding rock mass during tunnel excavation in rich water mountainous area.

2. Materials and Methods

2.1. Samples preparation

Fine-grained granite from Western China is selected as the test object, and the international standard cylindrical rock sample with size of is adopted, (see Figure.1). The wave velocity of each specimen was measured using an NM-48 ultrasonic analyser, and the rock sample was screened. The density, wave velocity, water content, and other basic physical parameters of a standard size rock samples are determined according to relevant specifications (see Table. 1).

Table. 1 shows that the average density of the rock is 2.78 $g \cdot cm^{-3}$; average longitudinal wave velocity is 3.99 $km \cdot s^{-1}$; average value of the natural water content is 0.07%; and average water absorption is 0.11%. The few pores in the rocks are small in size. The physical parameters of the rock samples approximate the mean values, thereby indicating that the rock samples are of good integrity and homogeneity.

Figure.1 Rock samples

Table.1 Basic physical parameters of rock samples

Number	Hight (mm)	Diameter (mm)	Density (g/cm^3)	Wave (km·s)	Moisture content (%)	Water absorption (%)
convention	100.55	49.02	2.76	3.97	0.07	0.11
S1	100.59	49.14	2.78	4.03	0.07	0.12
S2	100.58	49.20	2.80	4.03	0.08	0.12
S3	100.53	49.12	2.77	3.97	0.08	0.13
S4	100.57	49.11	2.79	3.97	0.07	0.13

2.2. Test Plan

Numerous methods are used in the unloading process of confining pressure. (1) When the bias voltage remains constant, the axial pressure and confining pressure decrease. (2) The increase of bias pressure can be refined as follows: constant axial pressure, unloading confining pressure, or increasing axial pressure at a certain loading rate, thereby releasing the confining pressure. The unloading method of maintaining the axial pressure constant and unloading confining pressure is utilized to highlight the influence of pore pressure on the deformation and mechanical properties of rock samples in the unloading process. According to the actual situation of the rock samples, the initial preset value of the confining pressure is 45 MPa, the initial preset value of the axial pressure is 210 MPa, and the set value of the pore pressure is 5 MPa. To study the influence of pore water pressure on the deformation and mechanical properties of granite during unloading, four unloading stages were designed in the test, and the drain valve was opened when unloading to 35, 25, 15, and 5 MPa. The steps are as follows.

(1) The axial, confining, and pore water pressures are loaded simultaneously to make the rock sample reach the hydrostatic pressure state. The loading rate is 0.1 MPa/s in the stress control mode.

(2) When the hydrostatic pressure is stable for a certain period, axial compression is applied to the preset value of the axial compression, which is taken as 80% of the peak strength of the conventional triaxial test of the granite used in this study. After reaching the predetermined value, the axial compression becomes stable and the loading rate is 0.1 MPa/s in the stress control mode.

(3) When unloading confining pressure and unloading at different stages, the drainage valve is opened until the specimen is damaged. The unloading rate is 0.03 MPa/s in the stress control mode.

3. Analysis of test results

3.1. Characteristics of Conventional Triaxial Stress-Strain

Figure 2 shows the stress–strain curves of the rock sample under a conventional triaxial compression test. The triaxial compressive strength used in the test is 262.8 MPa at a confining pressure level of 45 MPa. Therefore, 80% of the triaxial compressive strength, 210 MPa is selected as the initial axial pressure preset value of the unloading test.

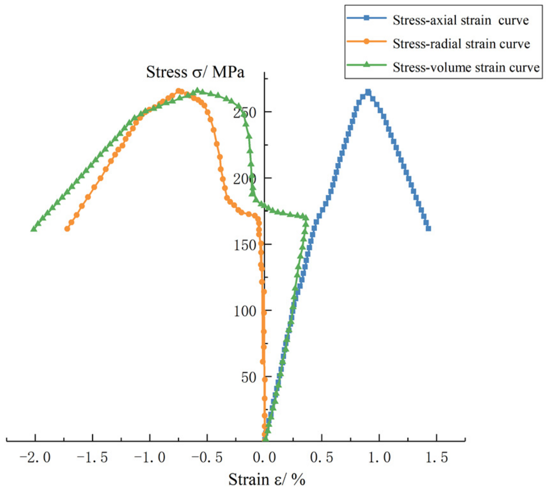

Figure. 2 Conventional triaxial stress-strain curves

3.2. Stress Strain Characteristics of Conventional Triaxial Unloading Test

Figure 3 shows the stress–strain curves of the rock sample under conventional triaxial unloading test. When the confining pressure is 45 MPa and the initial axial pressure is 210 MPa, the unloading stress–strain curve is consistent with the loading process curve. The axial, circumferential, and volume deformations caused by unloading confining pressure are greater than those under conventional loading. This result indicates that the fracture deformation of the rock sample caused by unloading confining pressure is substantially intense. The failure of the rock sample caused by unloading confining pressure is characterized as brittle failure, and the bearing capacity decreases rapidly with an increase in deformation.

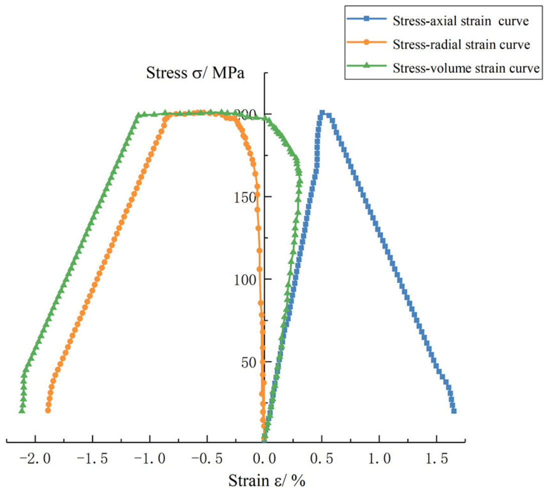

Figure. 3 Triaxial stress-strain curves of conventional unloading

3.3. Triaxial Unloading Stress-Strain Characteristics of Granite Under Pore Pressure

Figures 4 to 7 show the curves of the deviatoric stress versus the axial, circumferential, and volumetric strains after opening the pore pressure drainage valve when unloading to four different levels. The analysis is as follows.

(1) Under the influence of different pore pressures, the deformation law of the unloading stress–strain curve of fine-grained granite is similar. Owing to the low pore pressure in the static water, no evident deformation is observed in the pore pressure stage. During the loading process, the rock sample is in the elastic deformation stage, and the stress–strain curve is nearly a straight line. After

unloading under confining pressure, the deformation rate of the axial deformation decreases, while the ring deformation increases rapidly. When unloading reaches the failure stage, the principal stress difference decreases rapidly, the strain increases, and the unloading rock sample shows brittle failure.

(2) After unloading to different levels of confining pressure, pore pressure has an evident effect on the stress–strain curve of rock samples. When the confining pressure is released to 35 MPa, the axial strain is 0.015% and the circumferential strain is −0.02%. When the confining pressure is released to 5 MPa, the axial and circumferential strains are 0.015% and −0.026%, respectively. Evidently, water flow promotes the opening and development of fractures owing to the effects of pore pressure in the unloading fracture. It can cause an increase in the fracture opening in rock sample and even cause the initiation and development of new pores and fractures. These results lead to an increase in the lateral expansion deformation of the rock samples but have minimal effects on axial deformation.

(3) When the confining pressure is released to 35, 25, 15, and 5 MPa, the triaxial compressive strengths obtained by opening the pore pressure drainage valve are 199.56, 198.45, 196.49, and 193.18 MPa respectively. This result shows that the bearing capacity of the rock sample decreases owing to the influence of pore pressure after cracks are formed in unloading confining pressure. However, the test results indicate that the influence is not evident.

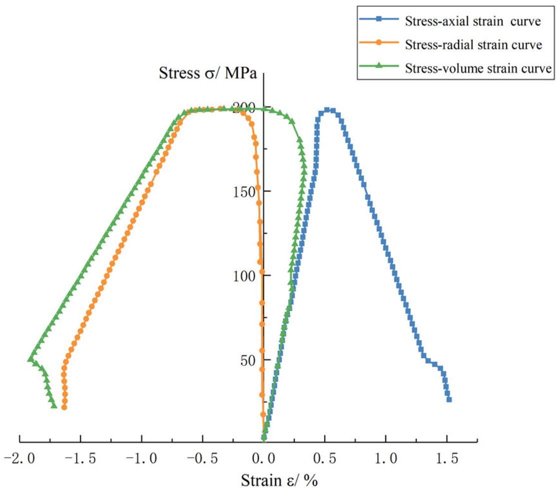

Figure.4 Stress strain curves after unloading to 35MPa and opening drain valve

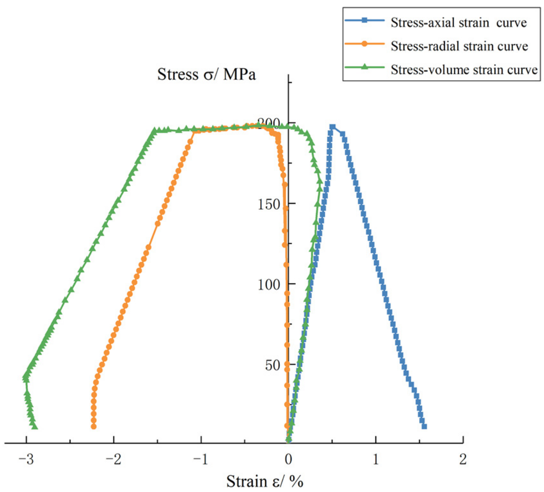

Figure.5 Stress strain curves after unloading to 25MPa and opening drain valve

IOP Conf. Series: Earth and Environmental Science **643** (2021) 012020 doi:10.1088/1755-1315/643/1/012020

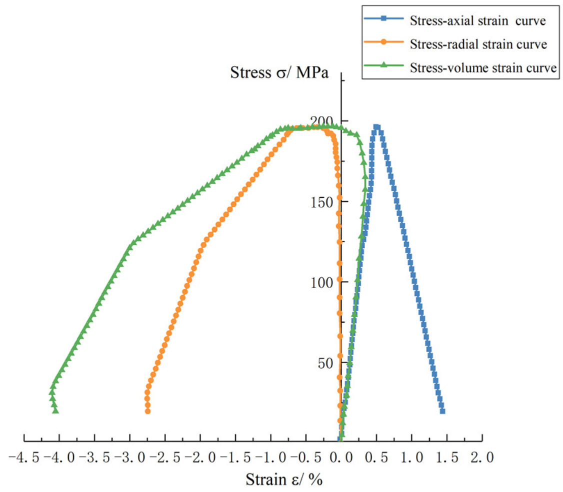

Figure.6 Stress strain curves after unloading to 15MPa and opening drain valve

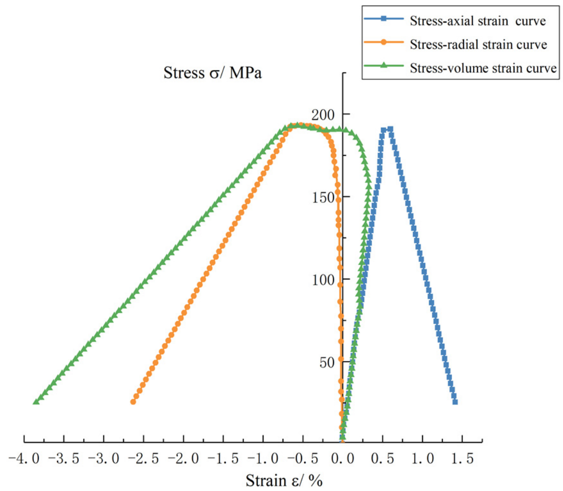

Figure.7 Stress strain curves after unloading to 5MPa and opening drain valve

3.4. Variation of Mechanical Parameters of Granite Under Pore Pressure

The deformation modulus and Poisson’s ratio are used to further study the influence of different unloading rates on the mechanical properties of rocks. Such as Equation (1).

$$\left.\begin{aligned} E &= (\sigma_1 - 2\mu\sigma_3)/\varepsilon_1 \\ \mu &= (B\sigma_1 - \sigma_3)/[\sigma_3(2B-1) - \sigma_1] \\ B &= \varepsilon_3/\varepsilon_1 \end{aligned}\right\} \tag{1}$$

Where E is the deformation modulus, μ is the Poisson's ratio and B is the ratio of radial strain to axial strain at the stage of confining pressure relief.

Figure 8 shows the curve of the granite deformation modulus and confining pressure obtained by opening the drain valve when the confining pressure is released to different orders of magnitude. Hence, the relationship between the deformation modulus and confining pressure of the rock samples in unloading confining pressure stage are approximately the same. At the beginning of unloading, the deformation modulus increases slightly. When unloading reaches 20 MPa, the deformation modulus of the rock samples decreases rapidly until they are destroyed. Moreover, the deformation modulus of the rock samples are evidently affected owing to the different action times of the pore and constant pressures. The deformation modulus of the rock samples decreases with an increase in action time.

This result shows that pore pressure at the initial stage can promote the mechanical properties of the rock samples in the process of unloading confining pressure. However, with an increase in unloading capacity, the internal cracks of rock increase and the effect of pore pressure on the rock samples have a significant deterioration. Consequently, the deformation modulus of the rock samples decreases rapidly, thereby leading to the failure of rock samples.

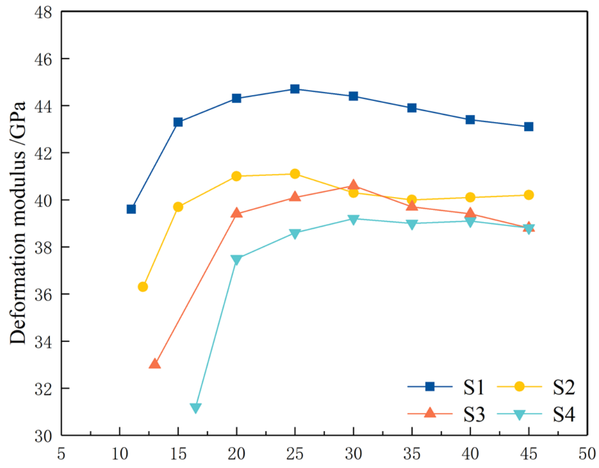

Figure.8 Relation curves between deformation modulus and confining pressure

Figure 9 shows the relationship between Poisson's ratio and confining pressure of granite after releasing this pressure to different orders of magnitude. The result shows that the initial Poisson's ratio of fine-grained granite is 0.2 to 0.3, and the changes in Poisson's ratio is small at the beginning of unloading confining pressure. When confining pressure is reduced to 20 MPa, evident radial deformation occurs and Poisson's ratio increases rapidly. Moreover, Poisson's ratio increases with an increase in unloading confining pressure, thereby indicating that the change in axial strain is smaller than that of the radial strain.

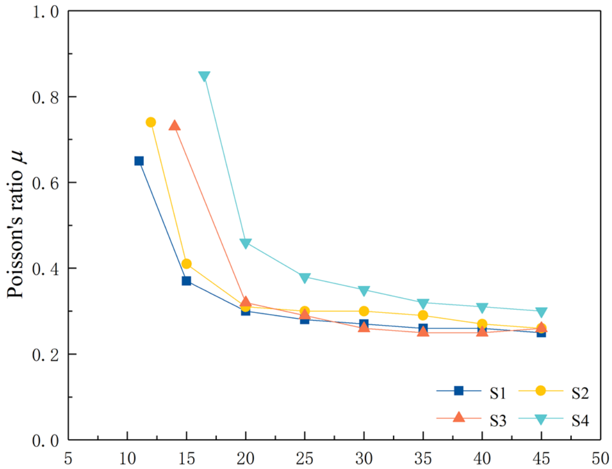

Figure.9 Relation curves between Poisson's ratio and confining pressure

3.5. Deformation Characteristics of Granite Under Pore Pressure

To intuitively describe the influence of pore pressure on the deformation process of the rock sample after releasing confining pressure to different orders of magnitude and opening the pore pressure drainage valve, the ratio of confining pressure relief to confining pressure relief can be expressed as Equation (2).

$$\dot{\varepsilon}_1 = \frac{\triangle \varepsilon_i}{\triangle \sigma_3} \tag{2}$$

Where $\triangle\varepsilon_i\left(i=1,3,V\right)$ expressed as axial strain, circumferential strain and volume strain increment.

Strain confining pressure compliance indicates the deformation speed of the axial, circumferential, and volume strains of the rock sample after unloading unit confining pressure. The influence of reducing confining pressure on deformation in the process of unloading confining pressure can be conveniently described. The larger the strain confining pressure compliance, the more evident the influence of unloading confining pressure on strain deformation in this direction. Figures 10 to 12 show the variation curves of the axial, circumferential, and volume strains corresponding to compliance when opening the pore pressure drainage valve after unloading to different confining pressure levels. It can obtained the following results.

(1) In unloading confining pressure, the variation law of unloading confining pressure and strain unloading confining pressure compliance curves are consistent. When the unloading confining pressure is below 5 MPa, the axial, annular, and volume strain unloading confining pressure compliance change rapidly. This result shows that the deformation of the rock sample increases at the beginning of the unloading confining pressure. With an increase of unloading confining pressure, the changes in axial, annular, and volume strain unloading confining pressure compliance are nearly the same. When the unloading confining pressure is between 5 MPa and 25 MPa, the rock sample is in stable deformation stage. When the unloading capacity reaches 25 MPa, the compliance of the strain relief confining pressure increases rapidly. After the unit confining pressure of the unloading unit, the rock sample deforms substantially, the internal fracture of the rock sample changes fundamentally, and the fracture develops continuously, thereby eventually leading to the failure of the rock sample.

(2) The compliance curves of the axial and circumferential strain unloading confining pressure relief of the rock samples indicate that the variation in the strain unloading confining pressure compliance of the rock samples is smallest during the conventional unloading process. In the curves from S1 to S4, the compliance of the strain relief confining pressure increases gradually, thereby indicating that pore pressure promotes the deformation of the rock samples. The results show that the deformation rate of the rock sample increases gradually, and the influence is significant.

(3) In the unloading process, pore pressure has an evident effect on the increment of the axial, circumferential, and volumetric strains, and the axial strain of the rock sample is smaller than that of the circumferential and volumetric strains. The results show that the response of pore pressure to circumferential and volumetric deformations is significant in the unloading process.

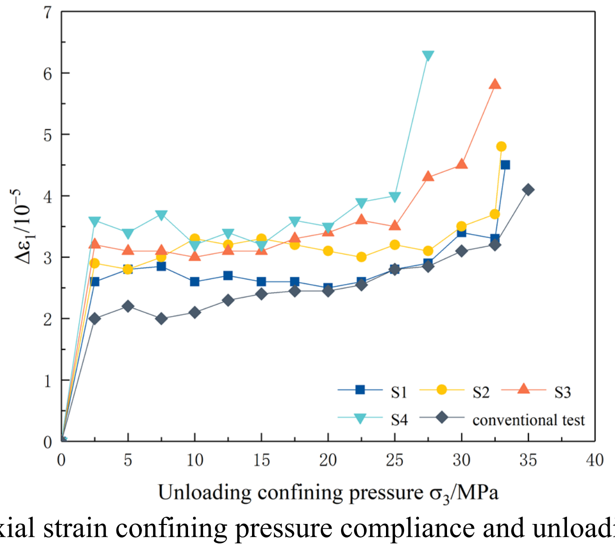

Figure.10 Curves of axial strain confining pressure compliance and unloading confining pressure

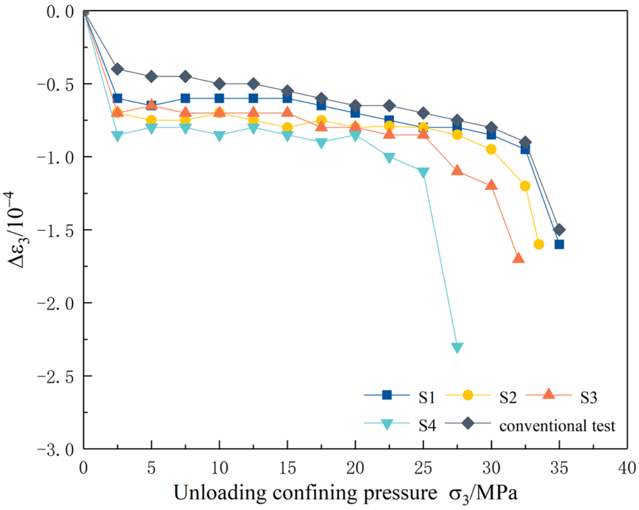

Figure.11 Curves of Radial strain confining pressure compliance and unloading confining pressure

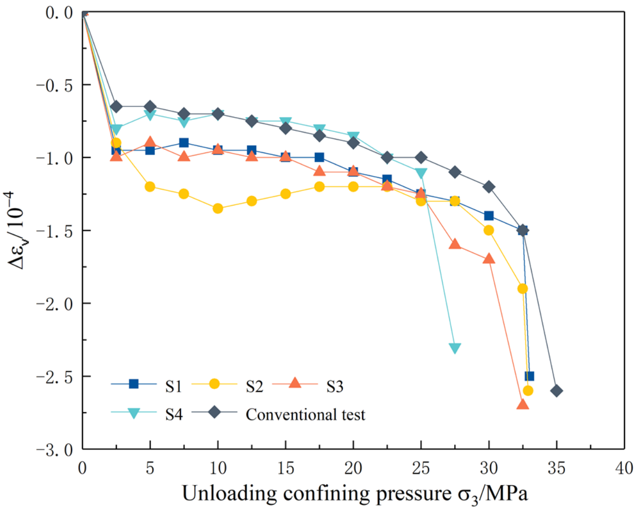

Figure.12 Volume strain confining pressure compliance and unloading confining pressure

3.6. Failure characteristics of rock sample under pore pressure

Figure 13 shows the failure and sketch the of rock sample under different pore pressures and under the condition of unloading confining pressure. This study presents the test results of opening the drain valve when the initial confining pressure is 45 MPa, when the initial confining pressure is 35, 25, 15, and 5 MPa. The deformation and failure law of rocks under different pore pressures is obtained. The analysis shown in Figures 13 to 16 present the following results.

(1) Under the initial confining pressure level of 45 MPa, pore pressure drainage valve was opened in the same magnitude, and the unloading test was performed under different pore pressure and constant pressure action times. The results show that the unloading failure of the rock sample is mainly shear failure, and evident tensile cracks are produced on the main failure shear plane trace.

(2) The fracture diagrams of the rock samples obtained from the four groups of tests indicate that the angle between the main fracture and horizontal line is the same with the different action times of the pore and constant pressures. When pore pressure is constant for a long time, numerous tension fractures are distributed around the main shear fracture during the fracture process owing to the influence of pore pressure on the fracture opening. The effect of pore pressure on the triaxial unloading failure mode of the rock samples is evident.

(3) The failure photos of the rock samples indicate that the increase in the action time of the constant pore pressure, the swelling phenomenon of the rock samples becomes increasingly evident. The results show that under the continuous action of pore pressure, the rock samples have evident circumferential deformation. These outcomes are consistent with the experimental results.

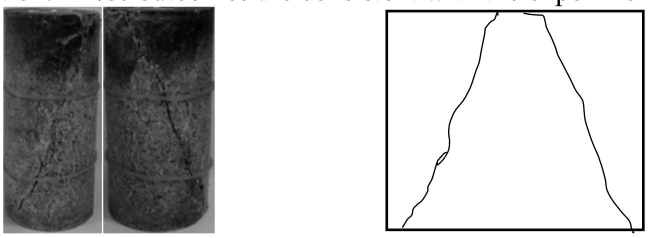

(a) Failure diagram of rock sample when opening drain valve at 35MPa.

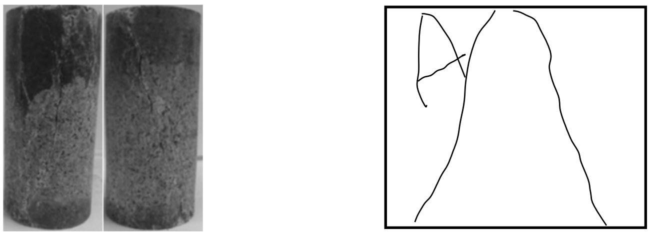

(b) Failure diagram of rock sample when opening drain valve at 25MPa.

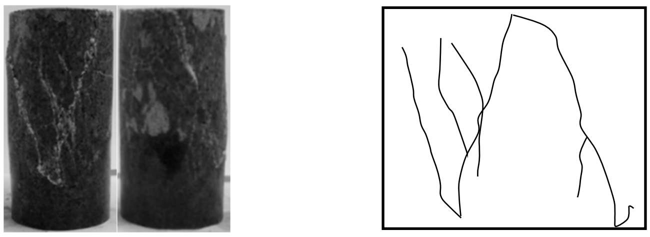

(c) Failure diagram of rock sample when opening drain valve at 15MPa.

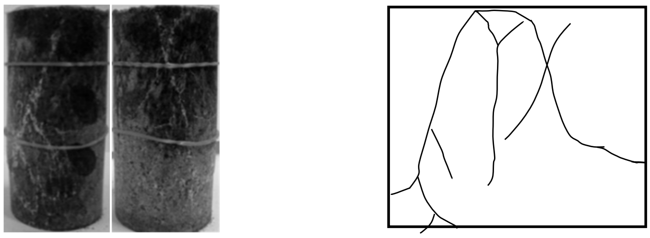

(d) Failure diagram of rock sample when opening drain valve at 5MPa.

Figure.13 The failure and sketch map of rock sample under different pore pressure.

4. Conclusion

Through the laboratory triaxial unloading confining pressure test performed in this study, the pore pressure drainage valve is opened after unloading to different orders of magnitude. The objective is to obtain the influence of pore pressure on the deformation law of fine-grained granite. The main conclusions are as follows:

- Under different pore pressures, the deformation law of the unloading stress–strain curve of fine-grained granite is similar. The stress–strain curve of fine-grained granite is approximately a straight line during axial compression loading, and the rock sample is at the elastic deformation stage. After unloading, the axial deformation rate decreases, but the circumferential deformation rate increases. After unloading, the principal stress difference decreases rapidly and the strain increases. In the process of unloading fracture, the lateral expansion deformation of the rock sample increases owing to the effect of pore pressure, and the axial deformation are minimally affected. The effect of pore water pressure reduces the bearing capacity of granite samples, but the influence is minimal based on the test results.

- In the process of unloading confining pressure, the variation law of unloading confining pressure and strain unloading compliance curves are consistent. When the unloading capacity is within 5 MPa, the deformation of the rock samples increases continuously. When the unloading amount is between 5 MPa and 25 MPa, the rock samples are in the stable deformation stage. When the unloading amount reaches 25 MPa, the unloading unit confining pressure will cause large deformations in rock samples, and fracture will continue to develop, eventually leading to rock samples failure. The pore pressure promotes the deformation of rock samples. When the pore pressure drainage valve are opened after different unloading amount, the deformation rate of rock samples increase gradually and the influence are significant. In the unloading process, the pore pressure has a substantial influence on radial deformation. That is, the response of the circumferential and volumetric deformations to pore pressure is significant.
- When the initial confining pressure level is 45 MPa, the pore pressure drainage valve is opened after unloading to different levels. When unloading test is conducted under different pore and constant pressures, the unloading failure of the rock samples are mainly shear failure. Therefore, under the condition of constant pore pressure for a long time, numerous tensile cracks are distributed around the main shear fracture during the fracture process of the rock samples owing to the influence of pore pressure on fracture opening. Given an increase in the time of the pore pressure constant pressure, the swelling phenomenon of the rock samples become increasingly evident. Lastly, the effect of triaxial compression on the failure of the rock samples are considerably evident.

Acknowledgements

This research was financially supported the National Natural Science Foundation of China (11872299) and the National Natural Science Foundation of China（12072259）

References

[1] Liu G, Zhao H J, Ma F S, et al.(2017).Research status and prospect of seepage stress coupling in fractured rock mass. National engineering geology report, Guilin.
[2] Yu J, Li H, Chen X, et al. (2013).Triaxial experimental study of associated permeability-deformation of sandstone under hydro-mechanical coupling. Chinese Journal of rock mechanics and engineering, 32 (6): 1203-1213.
[3] Hu D W, Zhu Q Z, Zhou H, et al. (2008). Research on anisotropic damage and permeability evolutionarylaw for brittle rocks . Chinese Journal of rock mechanics and engineering, 27(9): 1822-1827.
[4] Wei,P Egger,F Descoeudres.(1995).Permeability predictions for jointed rock masses," International Journal of Rock Mechanics & Mining Sciences & Geomechanics Abstracts, 32(3): 251-261.
[5] Hu D W, Zhou H, Xie S Y. et al. (2009) Research on nonlinear seepage characteristics and mechanism of post-peak marble. Chinese Journal of rock mechanics and engineering,28(3): 451-458.
[6] Zhu Z D, Zhang A J, Xu W Y. (2002) Experimental research on complete stress-strain process seepage characteristics of brittle rock.Rock and Soil Mechanics, 23(5): 555-558.
[7] Zhang L M, Ren M Y, Ma S Q, et al. (2016) Study on the physical-mechanical parameters of marble under different stress paths. Chinese Journal of underground space and engineering, 12 (5): 1288-1293, 1325.

[8] Min Ki-Bok,Rutqvist J,Tsang Chin-Fu, et al. (2004) Stress dependent permeability of fractured rock masses a numerical study. International Journal of Rock Mechanics and Mining Sciences, 41(7): 1191-1210.
[9] Huang R Q, Huang D. (2008) Study on deformation characteristics and constitutive model of rock On the condition of unloading. Advances in earth science, (05), 441-447,.
[10] Zhang C H, Zhao Q S, Wang L G, et al. (2015) Test and numerical modeling on strain softening behavior and permeability evolution of rock under triaxial compression. Journal of china coal society, 40(8), 1774-1782.
[11] Wang W, Xu W Y, Wang R B, et al. (2015) Permeability of dense rock under triaxial compression.Chinese Journal of rock mechanics and engineering, 34 (1), 40-47.
[12] Deng H F, Wang Z, Li J L, et al. (2017) Effect of unloading rate and pore water pressure on mechanical properties of sandstone. Journal of geotechnical engineering, 39(11), 1976-1983.
[13] LI Jing, PENG Cheng-le, Zhou H G, et al. (2017) Study on microscopic seepage characteristics of rocks based on microinfrared spectra technology. Chinese Journal of rock mechanics and engineering, (a01) , 3184-3191.
[14] Chen G Q, Jian D H, Xu P, et al. (2018)Energy characteristics of brittle failure of granite rock bridge under unloading compression. Journal of Engineering Geology, 26(03),602-610.
[15] Huang Y, Zhou L T, Zhou Z F.(2018)Equations for permeability variation of fractured rock mass under high water pressure. Journal of Engineering Geology,26(6),1433-1438.
[16] Mettam, G.R., Adams, L.B. (2009) How to prepare an electronic version of your article. In: Jones, B.S., Smith, R.Z. (Eds.), Introduction to the Electronic Age. E-Publishing Inc, New York. 281-304.
[17] Xie X S, Chen H S, Xiao X H, et al.(2019) Micro-structural characteristics and softening mechanism of red-bed soft rock under water-rock interaction condition. 27(05),pp.966-972.
[18] Li B Y, Liu J, Liu Z P, et al.(2002)The unloading mechanical properties of shale with different water saturation. Rock and Soil Mechanics, (S2), 1-11.
[19] Gao C Y, Xu J, He P et al.(2005)Study on mechanical property of marble under loading and unloading conditions. Chinese Journal of Rock Mechanics and Engineering, 24(3), 56-460.
[20] Qiu S L, Feng X T, Zhang C Q, et al. (2010) Experimental research on mechanical properties of deep-buried marble under different unloading rates of confining pressures. Chinese Journal of rock mechanics and engineering, 29(9), 1807-1817.